Testing violations of special and general relativity through the energy dependence of $\nu_\mu \leftrightarrow \nu_\tau$ oscillations in the Super-Kamiokande atmospheric neutrino experiment

G. L. Fogli, E. Lisi, A. Marrone, and G. Scioscia

Dipartimento di Fisica and Sezione INFN di Bari, Via Amendola 173, I-70126 Bari, Italy

The atmospheric neutrino data collected by the Super-Kamiokande experiment span about four decades in neutrino energy E, and are thus appropriate to probe the energy dependence of the oscillation wavelength λ associated with $\nu_\mu \leftrightarrow \nu_\tau$ flavor transitions, when these are assumed to explain the data. Such a dependence takes the form $\lambda^{-1} \propto E^n$ in a wide class of theoretical models, including "standard" oscillations due to neutrino mass and mixing ($n = -1$), energy-independent oscillations ($n = 0$), and violations of the equivalence principle or of Lorentz invariance ($n = 1$). We study first how the theoretical zenith distributions of sub-GeV, multi-GeV, and upward-going muon events change for different integer values of n. Then we perform a detailed analysis of the Super-Kamiokande data by treating the energy exponent n as a free parameter, with unconstrained scale factors for both the amplitude and the phase of $\nu_\mu \leftrightarrow \nu_\tau$ oscillations. We find a best-fit range $n = -0.9 \pm 0.4$ at 90% C.L., which confirms the standard scenario ($n = -1$) as the dominant oscillation mechanism, and strongly constrains possible concurrent exotic processes ($n \neq -1$). In particular, we work out the interesting case of leading standard oscillations plus subleading terms induced by violations of special or general relativity principles, and obtain extremely stringent upper bounds on the amplitude of such violations in the (ν_μ, ν_τ) sector. [S0556-2821(99)03115-X]

PACS number(s): 14.60.Pq, 04.80.Cc, 11.30.Cp, 96.40.Tv

I. INTRODUCTION

The recent atmospheric neutrino data from the Super-Kamiokande (SK) experiment [1] can be beautifully explained through flavor oscillations generated by nonzero neutrino mass and mixing [2,3] in the $\nu_\mu \leftrightarrow \nu_\tau$ channel [4]. Such an interpretation is consistent with all the SK data, including sub-GeV e-like and μ-like events (SG$e,\mu$) [5], multi-GeV e-like and μ-like events (MG$e,\mu$) [6], and upward-going muon events (UPμ) [7]. A combined analysis of the 33 kTy SK data sample can be found in [8]. The oscillation hypothesis has been strengthened by the latest (preliminary) 45 kTy SK data sample [9,10], and is also consistent with independent atmospheric neutrino results from the MACRO [11] and Soudan-2 [12] experiments, as well as with the finalized upward-going muon data from the pioneering Kamiokande experiment [13].

Establishing $\nu_\mu \leftrightarrow \nu_\tau$ oscillations generated by nonzero ν mass and mixing as the "standard" interpretation requires, however, further data and analyses. Basically, the following three aspects should be clarified: (1) the periodicity, (2) the flavors, and (3) the dynamics.

So far, the periodicity of the ν_μ oscillation pattern has not been experimentally observed in the neutrino energy (E) or path length (L) domain, and it is unlikely to emerge from the SK lepton distributions, largely smeared in energy or angle. Although specific nonperiodic scenarios, such as neutrino decay [14], can be indirectly excluded by careful analyses of SK data [15,16], the direct observation of a periodic disappearance pattern of ν_μ's remains an important goal for future atmospheric and long-base-line neutrino experiments.

In addition to periodicity, one should also identify unambiguously the flavor(s) of the oscillating partner(s) of ν_μ's because, in principle, all oscillation channels into active or sterile neutrinos might be open ($\nu_\mu \leftrightarrow \nu_\tau$, $\nu_\mu \leftrightarrow \nu_e$, $\nu_\mu \leftrightarrow \nu_s$). While the amplitude of possible $\nu_\mu \leftrightarrow \nu_e$ transitions is bound to be small [8], one cannot exclude $\nu_\mu \leftrightarrow \nu_s$ oscillations with a large amplitude with present SK data [9,10]. However, based on the fact that different oscillation channels induce somewhat different energy-angle lepton distributions, there are good prospects for a significant ($> 3\sigma$) discrimination of $\nu_\mu \leftrightarrow \nu_\tau$ from $\nu_\mu \leftrightarrow \nu_s$ with future SK data [17].

In this work we assume that both the periodicity (i.e., the existence of an oscillation length λ) and the oscillating flavors (ν_μ, ν_τ) are established, and we rather focus on the third aspect to be clarified: the dynamical origin of $\nu_\mu \leftrightarrow \nu_\tau$ oscillations. The standard oscillation dynamics, involving a nontrivial 2×2 neutrino mass matrix, leads to a well-known energy dependence of λ,

$$\lambda^{-1} \propto E^{-1} \quad (\text{standard}). \tag{1}$$

However, possible nonstandard neutrino interactions or properties can also generate (or coexist with) $\nu_\mu \leftrightarrow \nu_\tau$ oscillations [18,19]. An incomplete list of possibilities include violations of the equivalence principle (VEP) [20,21], flavor-changing neutral current (FCNC) (see [22] and references therein), neutrino couplings to space-time torsion fields [23], neutrino interactions through charged scalar particles [24], nonrelativistic heavy neutrinos [25], and violations of Lorentz invariance (VLI) [26,27] and of *CPT* symmetry [28]. In several such models the energy dependence of λ takes a power-law form [29]

$$\lambda^{-1} \propto E^n \quad (n \neq -1, \text{nonstandard}). \tag{2}$$

Although models with exotic dynamics for $\nu_\mu \leftrightarrow \nu_\tau$ oscillations do not survive Occam's razor, they might survive experimental tests. Effective tests must cover the widest pos-

sible energy range, as evident from Eqs. (1) and (2). Concerning atmospheric neutrinos, pre-SK data analyses covered only about two decades in energy (i.e., the so-called contained events, $E \sim 0.1$–10 GeV), and were compatible with several nonstandard scenarios, in particular with the VEP hypothesis (corresponding to $n=1$) [30,31]. An interesting post-SK analysis, covering a slightly more extended energy range [32], does not appear to discriminate significantly the three cases $n=0$ and $n=\pm 1$ examined. However, as observed in [15,16], a much longer "lever arm" in the energy domain is provided by the inclusion of partially contained and upward-going muon events (up to $E \sim 10^3$ GeV), thus providing a powerful tool to test exotic scenarios (which, indeed, appear to be disfavored in general [15]).

In this work we assess quantitatively the situation for $\nu_\mu \leftrightarrow \nu_\tau$ models with a power-law energy dependence of the oscillation length ($\lambda^{-1} \propto E^n$), including, as relevant subcases, standard mass-mixing oscillations ($n=-1$) and violations of the equivalence principle or of Lorentz invariance ($n=1$). We obtain two basic results: (1) The 90% C.L. range of n is determined to be $n=-0.9 \pm 0.4$, which is in striking agreement with standard oscillations, and excludes all $n \neq -1$ models as dominant sources of $\nu_\mu \leftrightarrow \nu_\tau$ transitions; (2) assuming the $n=1$ case as a subleading mechanism (coexisting with leading standard oscillations), we place stringent upper bounds on its amplitude. Such bounds can be interpreted as upper limits to violations of special or general relativity principles.

The plan of the paper is as follows. In Sec. II we analyze models with generic $\lambda^{-1} \propto E^n$ behavior, and constrain n through fits to SK atmospheric ν data. In Sec. III we consider a more complicated case with two coexisting sources for oscillations, namely, neutrino masses and violations of relativity principles. We summarize our results in Sec. IV.

II. ANALYSIS OF MODELS WITH $\lambda^{-1} \propto E^n$

In this section, we first review some oscillation models with λ depending on E through a power law. Then, independently of specific models, we study the phenomenology of atmospheric ν's, and constrain the energy exponent n through detailed fits to the SK data.

A. Review of models

Typical two-flavor Hamiltonians for $\nu_\mu \leftrightarrow \nu_\tau$ oscillations predict a flavor transition probability of the form

$$P(\nu_\mu \leftrightarrow \nu_\tau) = \sin^2 2\xi \, \sin^2(\pi \lambda^{-1} L), \qquad (3)$$

where ξ is the rotation (mixing) angle between the flavor basis and the basis where the Hamiltonian is diagonal, L is the neutrino path length, and λ is the neutrino oscillation length. In several cases of interest, λ depends on the neutrino energy E as [29,32]

$$\lambda^{-1} \propto E^n, \qquad (4)$$

with the exponent n taking integer (positive or negative) values.

For instance, the cases $n=-1$, 0, and 1 arise, respectively, in the presence of neutrino interactions mediated by scalar, vector, and tensor fields [32]. Specific models include

$$\lambda^{-1} = \frac{\Delta m^2}{4\pi E} \quad (n=-1, \text{ standard oscillations } [2]) \qquad (5a)$$

$$= \frac{E|\phi|\Delta\gamma}{\pi} \quad (n=1, \text{ violations of equivalence}$$

$$\text{principle } [20]) \qquad (5b)$$

$$= \frac{E\delta v}{2\pi} \quad (n=1, \text{ violations of Lorentz invariance } [26])$$

$$\qquad (5c)$$

$$= \frac{\delta b}{2\pi} \quad (n=0, \text{ violations of } CPT \text{ symmetry } [28])$$

$$\qquad (5d)$$

$$= \frac{Q\delta k}{2\pi} \quad (n=0, \text{ nonuniversal coupling to a}$$

$$\text{torsion field } [23]). \qquad (5e)$$

Standard oscillations [Eq. (5a)] are simply generated by nonzero neutrino masses ($\Delta m^2 = m_2^2 - m_1^2$), with a mixing angle ξ [Eq. (3)] usually denoted as θ_{23}, ψ, or simply θ (we adopt the symbol ψ in the following, as we use θ for the lepton zenith angle). In this case, the energy exponent is $n = -1$.

Equation (5b) refers to possible violations of the equivalence principle [20], namely, to nonuniversal couplings of neutrinos to the gravitational potential ϕ. The difference in such couplings is usually denoted by $\Delta\gamma$ and the mixing angle by θ_G. The potential seems to be dominated by the local supercluster ($\phi \sim 3 \times 10^{-5}$ [33]), but ambiguities in its definition suggest to use the product $\phi\Delta\gamma$ as a single, dimensionless free parameter, rather than ϕ and $\Delta\gamma$ separately (see [31,34,35] for recent discussions). The energy exponent of VEP-induced oscillations is $n=1$.[1]

Equation (5c) refers to possible violations of Lorentz invariance, namely, to asymptotic neutrino velocities different from c [26]. The parameter δv represents the speed difference in units of c. The mixing angle is usually denoted as θ_V. Since the energy exponent n is the same ($=1$) in both the VEP and VLI scenarios, such mechanisms are phenomenologically equivalent through the substitutions $|\phi|\Delta\gamma \rightarrow \delta v/2$ and $\theta_G \rightarrow \theta_V$ [27].

Equation (5d) refers to possible violations of the CPT symmetry through a more general class of Lorentz-violating

---

[1]An alternative, string-inspired VEP mechanism [36], leading to an energy exponent $n=-1$ rather than $n=1$, has been recently considered in [37]. Its phenomenology would be indistinguishable from the standard case, as far as $\nu_\mu \leftrightarrow \nu_\tau$ oscillations are involved. We do not consider such a VEP scenario in this work.

perturbations [28], δb being proportional to the *CPT*-odd Hamiltonian producing energy-independent ($n=0$) oscillations. It is interesting to notice that the most general Hamiltonian considered in [28] encompasses the three scenarios with $n=-1$, 0, and 1. See also [38] for the theory and tests of *CPT* and Lorentz-violating extensions of the standard model.

Finally, Eq. (5e) refers to possible nonuniversal couplings ($\Delta k \neq 0$) of neutrinos to a space-time torsion field of strength Q [23], which also produce energy-independent oscillations.

In principle, several oscillation mechanisms with different n's might occur at the same time, with corresponding complications in the analysis. In the next two subsections, however, we consider only one mechanism at a time. We will discuss the interesting case of coexisting $n=-1$ plus $n=+1$ oscillations in Sec. III.

A remark is in order. Not all "exotic" models for $\nu_\mu \leftrightarrow \nu_\tau$ transitions can be parametrized as in Eqs. (3) and (4). An important exception is represented by FCNC-induced oscillations (see [22] and references therein). In fact, although the FCNC oscillation phase is energy independent ($n=0$), it is proportional to the column density of electrons rather than to L. Therefore, FCNC-induced oscillations deserve a separate analysis [22,15] and will be considered in a future work. However, some features of the $n=0$ case also apply qualitatively to the FCNC case.

Finally, we note in passing that the analysis of nonstandard energy dependences for ν oscillations has some correspondence in the neutral kaon system, where the role of λ is played by the effective $K^0-\bar{K}^0$ mass difference (see [39] and references therein).

B. Model-independent analysis

In this section we do not commit ourselves to any specific model, and rather analyze the phenomenology of the $\lambda^{-1} \propto E^n$ dependence in the most general way. We assume that the $\nu_\mu \leftrightarrow \nu_\tau$ oscillation probability takes the form

$$P(\nu_\mu \leftrightarrow \nu_\tau) = \alpha \sin^2\left(\beta \frac{L}{10^3 \text{ km}} \frac{E^n}{\text{GeV}^n}\right), \qquad (6)$$

where α is an overall scale factor ($0 \leq \alpha \leq 1$) for the oscillation amplitude, β is an unconstrained scale factor for the oscillation phase, and n is a free exponent (not necessarily equal to -1, 0, or 1). The units in Eq. (6) have been conveniently chosen on the basis of the current Super-Kamiokande data, which suggest an oscillation length of $O(10^3$ km) for neutrino energies of $O(1$ GeV). The standard oscillation case is recovered by taking $n=-1$, $\alpha=\sin^2 2\psi$, and $\beta=1.27 \Delta m^2/(10^{-3} \text{ eV}^2)$.

Equation (6) is used to calculate the observable rates of sub-GeV, multi-GeV, and upward through-going muon events in SK as a function of the lepton zenith angle θ, using the same detailed and accurate approach as in Refs. [8,16], to which we refer the reader for technical details. Here we just remind the reader that the parent neutrino distributions for sub-GeV (SG), multi-GeV fully contained (MG FC), multi-
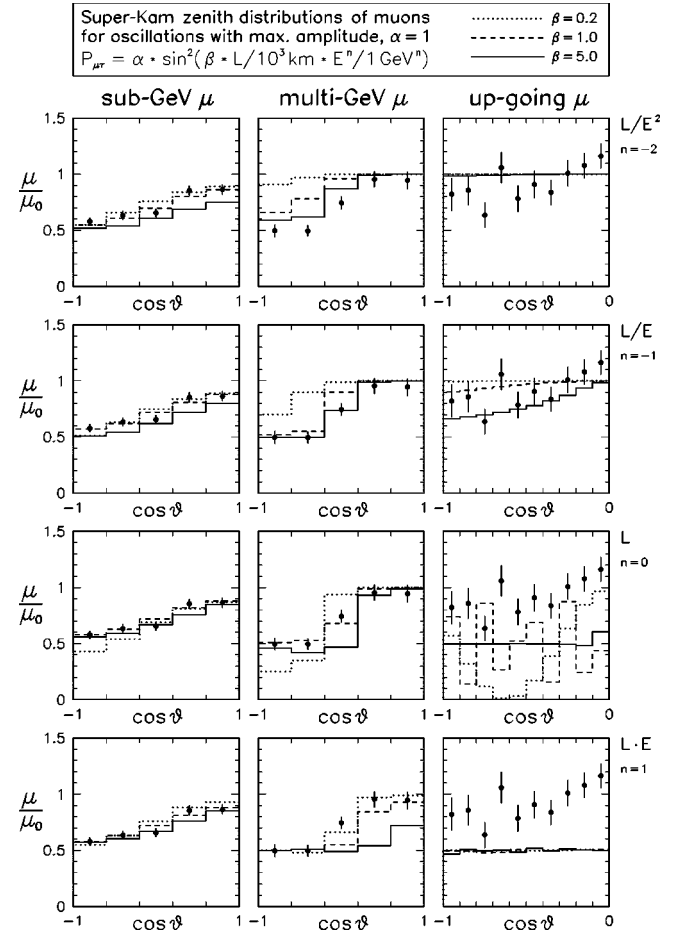

FIG. 1. Expected zenith distributions of SGμ, MGμ, and UPμ events in Super-Kamiokande for maximal mixing ($\alpha=1$) and for representative values of β: dotted line, $\beta=0.2$; dashed line, $\beta=1$; solid line, $\beta=5$. In each bin, the muon rates μ are normalized to the expectations μ_0 in the absence of oscillations. The 45 kTy SK data (dots with statistical error bars) are superposed to guide the eye. From top to bottom, the energy exponent n takes the values $n=-2,-1,0$, and 1.

GeV partially contained (MG PC), and upward through-going (UP) muon events are roughly distributed in the ranges 0.1–3 GeV, 1–10 GeV, 1–10^2 GeV, and 10–10^3 GeV, respectively, thus covering about four decades in E.

Figure 1 shows the expected zenith distributions of SGμ, MGμ (FC+PC), and UPμ events in Super-Kamiokande for maximal mixing ($\alpha=1$) and for three representative values of β: dotted line, $\beta=0.2$; dashed line, $\beta=1$; solid line, $\beta=5$. In each bin, the muon rates μ are normalized to the expectations μ_0 in the absence of oscillations, so that deviations from the no-oscillation case ($\mu/\mu_0=1$) are immediately recognizable. Since we are considering pure $\nu_\mu \leftrightarrow \nu_\tau$ oscillations ($e/e_0=1$ always), the electron rates are not shown. The effect of taking $\alpha<1$ can be approximately described by reducing proportionally the amount of muon disappearance in each subfigure. The theoretical expectations are affected by relatively large and strongly correlated uncertainties (not shown), mainly related to the overall normalization of the atmospheric neutrino flux [8]. The 45 kTy SK

data [9,10] (dots with statistical error bars) are superposed to guide the eye, although no fit to the data is implied by this figure.

In Fig. 1, from top to bottom, the energy exponent n takes the values $n = -2, -1, 0$, and 1, corresponding to a dependence of the kind L/E^2, L/E, L, and $L \cdot E$ for the oscillation phase. Such four cases are described in the following.

Case L/E^2. This case ($n = -2$) does not correspond to any known model, and is used only to extend the study to a power-law energy dependence faster than in the standard case ($n = -1$). The muons appear to be significantly suppressed at the lowest (SG) energies, the more the larger β. An excessive suppression of SG muons is avoided only by keeping $\beta \lesssim 1$. On the other hand, such values of β are too low to produce a significant suppression of MG muons, which rather prefer $\beta \gtrsim 5$. Therefore, one expects a "compromise" between underestimated SGμ rate and overestimated MGμ rates for β in the range ~ 1–5. UPμ events are basically unsuppressed, due to their high energy. Reducing α would be of no help in reducing the conflict between SG and MG muon expectations.

Case L/E. This is the "standard" oscillation case, which, as well known, provides an excellent description of the SK data for $\Delta m^2 \sim$ few$\times 10^{-3}$ eV^2 [4,8]. Therefore, it is not surprising to see in Fig. 1 that, for values of β in the range ~ 1–5, all the muon data are well reproduced. Higher values of β would suppress SG muons too much, while lower values would not produce enough suppression at higher energies (MGμ and UPμ samples).

Case L. In this case, the ν_μ survival probability is energy independent, and the differences in the muon suppression patterns among the SG, MG, and UP muon samples are mainly due to the different angular smearing. At low (SG) energies the smearing is very effective and there is little difference between the three curves, while higher-energy, MG muons are more discriminating. Values of β around unity (dashed curve) seem to be preferred by SG+MG data, and produce a significant ($\sim 1/2$) suppression below the horizon. UP muons have a different suppression pattern, which is highly correlated with the parent neutrino direction, and follows closely the variations of $P_{\mu\mu}$ with L (dashed and dotted curves), until the oscillations are so fast to be unresolved within the bin width (solid curve). The expected UPμ suppression appears to be larger than suggested by the data, unless α is taken to be nonmaximal; however, for $\alpha < 1$ the relatively good description of SG+MG data would be spoiled (not shown).

Case $L \cdot E$. In this case, the ν_μ survival probability rapidly approaches the average value 1/2 as the energy increases. Therefore, although SG+MG data can be described relatively well with $\alpha = 1$ and $\beta \sim 0.2$, the expected UPμ rates are too low in any case. As in the previous $n = 0$ scenario, taking $\alpha < 1$ would help to reproduce the UPμ data, but would worsen the description of SG+MG data. No satisfactory compromise can be reached.

In all four cases, it can be seen that SG (or even SG+MG) data alone do not discriminate strongly among the various scenarios, since they do not probe the full energy range explorable by SK. This might explain why the

SG+MG analysis in [32] could not significantly distinguish the three cases $n = -1, 0$, and 1. The inclusion of UPμ data extends the range up to $E \sim 10^3$ GeV, and provides a very important tool to probe the energy dependence of λ [15].

In conclusion, from the examination and the comparison of the oscillated muon distributions at different values of n shown in Fig. 1, the case $n = -1$ emerges as a good description of the SK data at all energies, while for $n \neq -1$ the patterns of muon suppression at low (SG), intermediate (MG), and high (UP) energies appear to be in conflict with the data.

C. Fits to the Super-Kamiokande data

The qualitative understanding of the muon distributions at different values of n (previous subsection) can be improved by performing quantitative fits to the 45 kTy preliminary SK data [9,10]. We use a χ^2 approach that, as described in [8], takes into account several sources of correlation among the systematics affecting the theoretical predictions. Even if ν_e's do not participate in oscillations in the scenarios considered here, we have included the SG and MG e-like data in the analysis (for a total of 30 data points), since they play an important role in constraining the overall normalization uncertainty (see also [8,16]).

Figure 2 shows the best-fit zenith distributions of muons for the four cases considered in Fig. 1 ($n = -2, -1, 0$, and 1), as obtained by leaving α and β unconstrained. The values of α, β, and χ^2 at the best-fit points are reported in the top part of the figure. The L/E ($n = -1$) case provides an excellent fit to the data ($\chi^2_{\min}/N_{DF} = 20.3/28$), while all the other cases do not provide a good description of at least one data sample (SGμ, MGμ, or UPμ). In particular, for $n = -2$ there is insufficient up-down asymmetry of MGμ's and no slope of UPμ's; for $n = 0$ none of the zenith distributions is correctly reproduced; for $n = 1$ there is a too strong and flat suppression of UPμ's.

In Fig. 3 we present the χ^2 curve as obtained by taking also n as a free parameter, besides α and β. Although noninteger values of n may not be related to any realistic oscillation dynamics, this exercise is useful to see how accurately n is determined through the SK data. The result is striking:

$$n = -0.9 \pm 0.4 \text{ at } 90\% \text{ C.L.} \qquad (7)$$

(corresponding to $\chi^2 - \chi^2_{\min} = 6.25$ for $N_{DF} = 3$). This narrow range for n is perfectly consistent with standard ($n = -1$) neutrino oscillations and inconsistent with any other integer value of n.

Given the importance of standard $\nu_\mu \leftrightarrow \nu_\tau$ oscillations, we show in Fig. 4 the updated limits on the oscillation parameters Δm^2 and $\sin^2 2\psi$. We find the best fit at $\Delta m^2 = 2.8 \times 10^{-3}$ eV^2 and maximal mixing. The bounds in Fig. 4 are in good agreement with the latest full data analysis from the SK Collaboration [10].

In conclusion, standard oscillations ($\lambda^{-1} \propto E^{-1}$) are strongly favored as the *dominant* mechanism for the $\nu_\mu \leftrightarrow \nu_\tau$ flavor transitions of atmospheric neutrinos in SK. Alternative mechanisms of the kind $\lambda^{-1} \propto E^n$ (with $n \neq -1$) *cannot* be
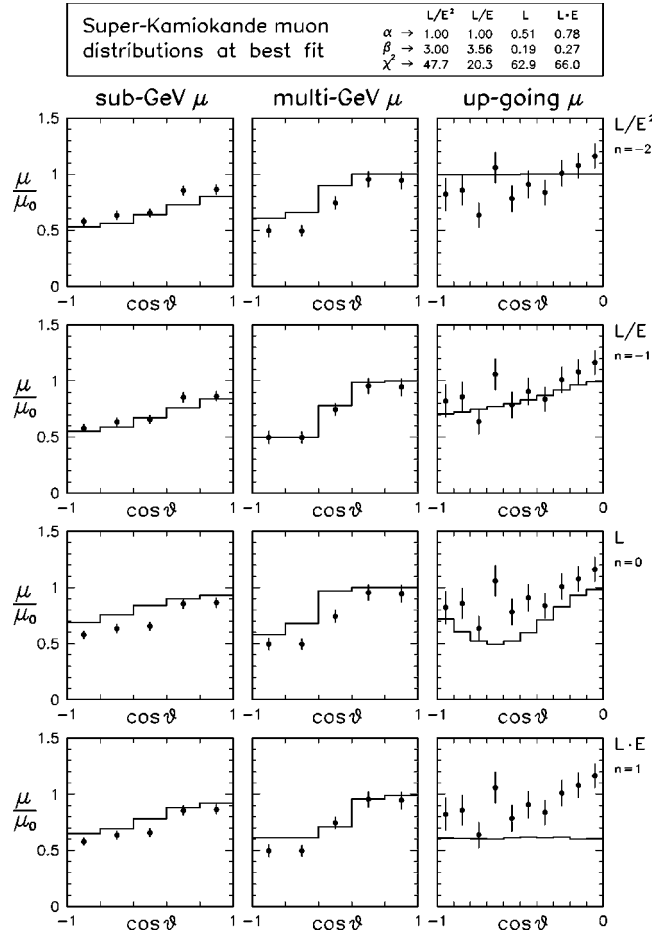
FIG. 2. Best fits to the zenith distributions of muons in SK for the four cases considered in Fig. 1 ($n = -2$, -1, 0, and 1), as obtained through a χ^2 analysis of all the data (μ-like and e-like events) with unconstrained α and β. The values of α, β, and χ^2 at the best-fit points are reported in the top part of the figure.

the dominant source of the muon disappearance in SK. In particular, violations of special or general relativity principles (VLI or VEP, leading to $\lambda^{-1} \propto E$) cannot explain the bulk of SK atmospheric ν data. Therefore, if $n \neq -1$ oscillations occur in nature, they can only be subleading processes with small amplitude, coexisting with leading, large-amplitude $n = -1$ standard oscillations. Such results generalize and refine previous indications that SK data could disfavor some exotic models [15].

III. CONSTRAINTS ON VIOLATIONS OF RELATIVITY PRINCIPLES

In this section we consider a more complicated case, characterized by leading $n = -1$ oscillations plus subleading $n = +1$ oscillations, possibly generated by violations of relativity principles (VEP or VLI). We show that the fit to the SK data is not improved with respect to the case of standard $\nu_\mu \leftrightarrow \nu_\tau$ transitions. As a consequence, we derive upper bounds on such violations. A brief review of the theoretical formalism precedes the phenomenological analysis.
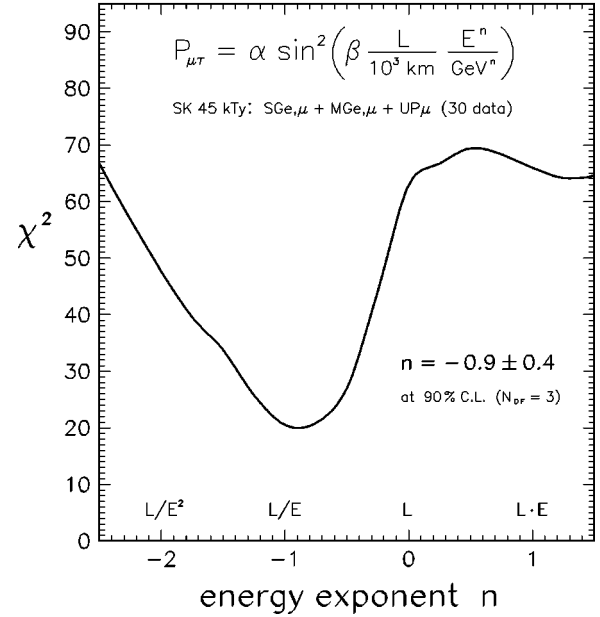

FIG. 3. χ^2 function from the fit to the SK data, assuming continuous values of the energy exponent n and unconstrained scale factors for the oscillation amplitude α and phase β. The standard case ($n = -1$) is very close to the best fit.

A. Violations of relativity principles: Formalism

The theory and phenomenology of neutrino violations of the equivalence principle [20] have been investigated in a Önumber of papers, including studies of the solar ν deficit [30,31,34,35,40–45], of the atmospheric ν anomaly [29–32],
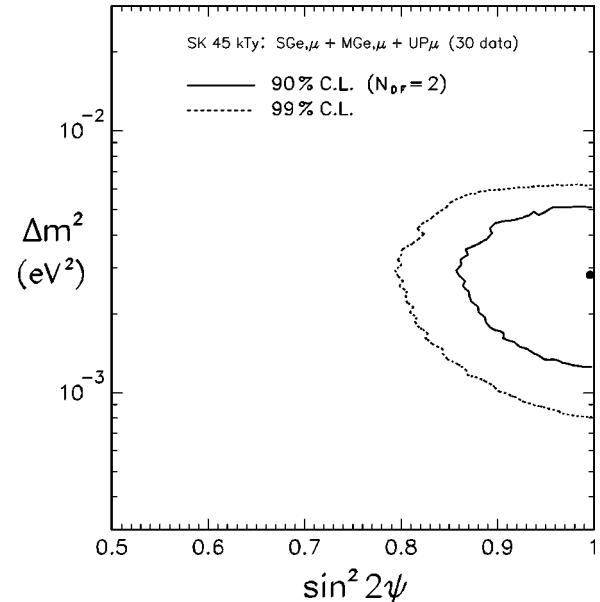

FIG. 4. Updated bounds on the neutrino mass-mixing parameters for standard $\nu_\mu \leftrightarrow \nu_\tau$ oscillations, as derived by our global analysis of all the Super-Kamiokande atmospheric neutrino data.

of oscillation searches at short base line [46] and long base line [29,31,47] accelerator facilities, and of double beta decay [48]. Given the phenomenological equivalence of violations of Lorentz invariance [26] and of the equivalence principle [27], neutrino oscillation searches can be generally interpreted as tests of fundamental principles of both special and general relativity, with a sensitivity at levels below 10^{-20} (see, e.g., [28,31]). Here we focus on the case of VEP- or VLI-induced oscillations coexisting with standard oscillations. Mixed scenarios of this kind have been considered, e.g., in [21,28,31,42] but to our knowledge, they have not been discussed on the basis of Super-Kamiokande atmospheric ν observations so far.

In the presence of several concurrent processes leading to $\nu_\mu \leftrightarrow \nu_\tau$ oscillations, the global Hamiltonian H is the sum of several 2×2 matrices H_n, which can be diagonalized through separate rotations (with angles ξ_n) of the flavor basis (ν_μ, ν_τ). As far as models of the kind $\lambda^{-1} \propto E^n$ are concerned, the rotation angle ξ, which diagonalizes the total Hamiltonian, is related to the oscillation length λ through equations of the form [28]

$$\pi \lambda^{-1} \sin 2\xi = \left| \sum_n c_n \sin 2\xi_n E^n e^{i\eta_n} \right|, \qquad (8a)$$

$$\pi \lambda^{-1} \cos 2\xi = \sum_n c_n \cos 2\xi_n E^n, \qquad (8b)$$

where the coefficients c_n parametrize the strength of each oscillation mechanism. In general, only one of the complex phase factors $e^{i\eta_n}$ can be rotated away, the others being physically observable [28,31]. For any given choice of the parameters (c_n, ξ_n, η_n), one has to derive the values of λ and ξ from the previous equations, and insert them in Eq. (3) to get the flavor transition probability.

In the specific case of standard+VEP ($n = -1 \oplus n = +1$) oscillations, Eqs. (8a) and (8b), can be rewritten as [31]

$$\pi \lambda^{-1} \sin 2\xi = \left| 1.27 \frac{\Delta m^2}{E} \sin 2\psi + 5.07 \frac{|\phi|\Delta\gamma}{10^{-21}} E \sin 2\theta_G e^{i\eta} \right|, \qquad (9a)$$

$$\pi \lambda^{-1} \cos 2\xi = 1.27 \frac{\Delta m^2}{E} \cos 2\psi + 5.07 \frac{|\phi|\Delta\gamma}{10^{-21}} E \cos 2\theta_G, \qquad (9b)$$

where the following units have been used: $[\Delta m^2] = 10^{-3}$ eV^2, $[L] = [\lambda] = 10^3$ km, and $[E] =$ GeV. The same equations formally apply to violations of Lorentz invariance, modulo the replacements $|\phi|\Delta\gamma \rightarrow \delta v/2$ and $\theta_G \rightarrow \theta_v$ [27]. Notice that the oscillation phase $\pi \lambda^{-1} L$, to be inserted in Eq. (3), is proportional to the geometric average of the right hand sides of the above equations, so it will contain, besides the standard term ($\propto E^{-1}$) and the VEP term ($\propto E$), also an energy-independent interference term. The oscillation amplitude $\sin^2 2\xi$ also acquires a nontrivial dependence on the neutrino energy through Eq. (9).

B. Constraints from Super-Kamiokande data

Before performing a detailed fit to the SK data in the standard+VEP oscillation scenario, let us derive some qualitative bounds on the magnitude of possible VEP terms. According to the conclusions of Sec. II, we expect that the second (VEP) term on the right hand of Eqs. (9a) and (9b) should be typically much smaller than the first (standard) term, namely

$$5.07 \frac{|\phi|\Delta\gamma}{10^{-21}} \frac{E}{\text{GeV}} \ll 1.27 \frac{\Delta m^2}{10^{-3}\text{ eV}^2} \frac{\text{GeV}}{E} \qquad (10)$$

or equivalently (for $\Delta m^2 \sim$ few$\times 10^{-3}$ eV^2)

$$|\phi|\Delta\gamma \ll 10^{-21} \left(\frac{\text{GeV}}{E} \right)^2. \qquad (11)$$

Therefore, the constraints to VEP effects should be stronger in the highest-energy SK data sample (UPμ events). Since the parent neutrino energy spectrum for UPμ's is peaked around 10^2 GeV, the sensitivity to VEP-induced oscillations is expected to reach levels of $O(10^{-25})$ in the parameter $|\phi|\Delta\gamma$ (or, equivalently, in the parameter $\delta v/2$ for the VLI case). Of course, such sensitivity depends somewhat on θ_G.

In order to get some insight into the θ_G dependence of the expected constraints, let us consider the extreme values $\theta_G = 0$ and $\theta_G = \pi/4$, and take $(\Delta m^2, \sin^2 2\psi)$ at their best-fit values $(2.8\times 10^{-3}$ eV$^2, 1)$. We also fix $e^{i\eta} = 1$ for simplicity. Then $P_{\mu\tau}$ takes a simple form

$$P_{\mu\tau} = \begin{cases} \dfrac{1}{1+x^2} \sin^2(A\sqrt{1+x^2}), & \theta_G = 0, \\ \sin^2[A(1+x)], & \theta_G = \pi/4 \end{cases} \qquad (12)$$

where $A = 3.56 L/E$, $x = 1.42 E^2 |\phi|\Delta\gamma/10^{-21}$, and the units are $[E] =$ GeV and $[L] = 10^3$ km. The standard case ($P_{\mu\tau}^{\text{std}} = \sin^2 A$) is recovered for $x = 0$. In the UPμ event sample, where the VEP effect is larger, the value of A is typically small ($\lesssim 0.6$), and one can easily check numerically [from Eq. (12)] that the difference $P_{\mu\tau} - P_{\mu\tau}^{\text{std}}$ grows more rapidly with x for $\theta_G = \pi/4$ than for $\theta_G = 0$. Therefore, we expect a higher sensitivity to x (i.e., to $|\phi|\Delta\gamma$) at larger θ_G. Moreover, at small values of both A and x it turns out that $P_{\mu\tau} - P_{\mu\tau}^{\text{std}} < 0$ (> 0) for $\theta_G = 0$ ($\theta_G = \pi/4$), so that the muon rates should be less (more) suppressed than in the standard oscillation case.

Figure 5 illustrates quantitatively the previous considerations, by showing the VEP effect (added to best-fit standard oscillations) on the SK muon distributions for two representative cases: (i) $\theta_G = 0$ and $|\phi|\Delta\gamma = 1.5\times 10^{-24}$ (solid line) and (ii) $\theta_G = \pi/4$ and $|\phi|\Delta\gamma = 2.0\times 10^{-26}$ (dotted line). We anticipate that such values are close to the border of the parameter region excluded by SK. The standard oscillation curves ($|\phi|\Delta\gamma = 0$) are also shown for reference (dashed lines); they are identical to the best fit curves for standard oscillations ($n = -1$) in Fig. 2. As expected from the pre-
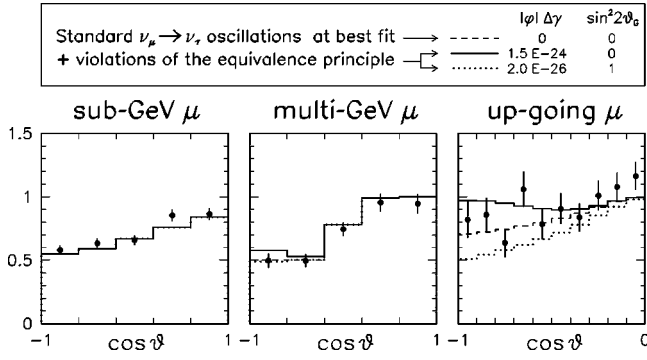
FIG. 5. Effect of subleading oscillations induced by violations of the equivalence principle on the muon distributions in Super-Kamiokande. Standard mass-mixing oscillation parameters are taken at their best fit, and the complex phase $e^{i\eta}$ is taken equal to 1. Dashed line: no VEP. Solid line: VEP with $|\phi|\Delta\gamma = 1.5\times10^{-24}$ and $\theta_G = 0$. Dotted line: VEP with $|\phi|\Delta\gamma = 2\times10^{-26}$ and $\theta_G = \pi/4$.

ceding discussion, the VEP effect is manifest at high energies (UPμ sample), and the expected deficit of UPμ's is more pronounced for $\theta_G = \pi/4$ than for $\theta_G = 0$.

The next step is to perform a χ^2 analysis of the standard +VEP scenario. We take for the moment $(\Delta m^2, \sin^2 2\theta) = (2.8\times10^{-3}\ \mathrm{eV}^2, 1)$ and $e^{i\eta} = 1$, while leaving the parameters $(|\phi|\Delta\gamma, \theta_G)$ free. We find an important result that strengthens the conclusions of Sec. II: The χ^2 fit is never improved in the presence of VEP effects, as compared with the value $\chi^2_{\min} = 20.3$ derived in Fig. 2 for the standard case. Thus, not only can VEP-induced oscillations not be the *leading* mechanism underlying the SK observations, but also there is no indication in favor of *subleading* VEP oscillation terms. As a consequence, we can place well-defined upper bounds on violations of relativity principles in the (ν_μ, ν_τ) sector.

Figure 6 shows the 90% and 99% C.L. limits on $|\phi|\Delta\gamma$ as a function of the VEP mixing parameter $\sin^2 2\theta_G$. The same limits apply to the neutrino asymptotic speed difference $\delta v/2$, as a function of the VLI mixing parameter $\sin^2 2\theta_v$. As expected from the discussion at the beginning of this subsection, the limits obtained in Fig. 6 are roughly of $O(10^{-25})$, and become stronger as θ_G increases. The stringent bounds in Fig. 6, together with the results shown in Fig. 3, represent our main contribution to the current understanding of atmospheric neutrino oscillations induced by violations of relativity principles in the (ν_μ, ν_τ) sector. Notice that such bounds preempt the region of VEP (or VLI) parameters explorable with proposed long-base-line accelerator neutrino facilities [31].[2]

Finally, we have investigated the robustness of the bounds shown in Fig. 6 under variations of the standard mass-mixing parameters. We have repeated the fit by varying Δm^2 and $\sin^2 2\psi$ within the 90% C.L. limits shown in Fig. 4 and also by taking negative values for $\Delta\gamma$, as well as generic values

_____

[2]Notice that the values of L, E, and $L \cdot E$ probed in the UPμ sample by Super-Kamiokande are higher than in proposed long-base-line neutrino beams.
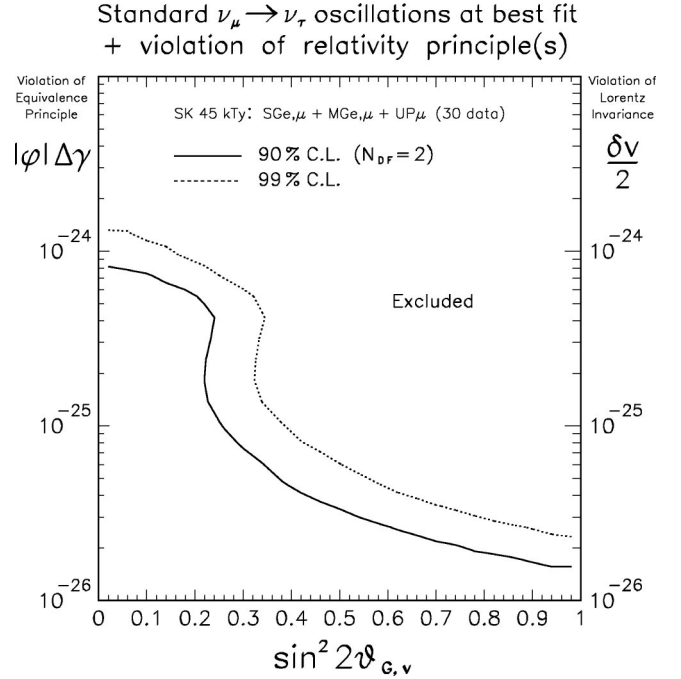

FIG. 6. Bounds on the parameters that characterize violations of special or general relativity principles, assumed to generate subleading $\nu_\mu \leftrightarrow \nu_\tau$ flavor transitions concurrent with standard (leading) neutrino oscillations. Best-fit neutrino mass-mixing values are assumed. See the text for further details.

for the complex phase η. We have found that, in any case, the value of $\chi^2_{\min}$ is not smaller than in the best-fit standard case. Therefore, standard+VEP (or standard+VLI) oscillations never represent a better description of the SK data, as compared to best-fit standard oscillations. Under the above variations, the upper bounds shown in Fig. 6 are somewhat modified within factors of a few, but do not change qualitatively: they always become stronger as $\sin^2 2\theta_G$ increases. The most conservative upper bound (including negative $\Delta\gamma$ cases) turns out to be

$$|\phi\Delta\gamma| < 3\times10^{-24} \text{ at } 90\% \text{ C.L.,} \tag{13}$$

independently of θ_G. In the specific case $\theta_G = \pi/4$, the above bound can be lowered at least to $\lesssim 10^{-25}$. Analogous limits apply to the VLI parameters $|\delta v|/2$ and θ_v. In particular,

$$|\delta v| < 6\times10^{-24} \text{ at } 90\% \text{ C.L.} \tag{14}$$

To our knowledge, the above limits to violations of special or general relativity principles are the strongest placed so far in the (ν_μ, ν_τ) sector. They are valid under an assumption which is supported by the present data and appears likely to be corroborated in the future, namely, that standard $\nu_\mu \leftrightarrow \nu_\tau$ oscillations generated by ν mass and mixing represent the dominant mechanism underlying the Super-Kamiokande observations.

IV. SUMMARY AND CONCLUSIONS

Among the $\nu_\mu \leftrightarrow \nu_\tau$ models with oscillation length following a power-law energy dependence, standard neutrino oscillations generated by ν mass and mixing are unique in providing a good description of the Super-Kamiokande atmospheric neutrino data, and are strongly favored as the leading mechanism for (ν_μ, ν_τ) flavor transitions. Additional, subleading $\nu_\mu \leftrightarrow \nu_\tau$ oscillations generated by possible violations of special or general relativity in the neutrino sector do not improve the agreement with the data, and must thus have a relatively small (or zero) amplitude. In particular, the fractional difference of asymptotic ν velocities $|\delta v|/2$ or of ν couplings to gravity $|\phi \Delta \gamma|$ cannot exceed the value $\sim 3 \times 10^{-24}$ at 90% C.L. for unconstrained neutrino mixing. The broadness of the neutrino energy range probed by Super-Kamiokande is crucial to obtain such strong limits.

[1] Y. Totsuka, in Proceedings of the 1998 Nobel Symposium Particle Physics and the Universe, Enkoping, Sweden, 1998, edited by L. Bergstrom, P. Carlson, and C. Fransson [Phys. Scr. (to be published)]; report available at http://www-sk.icrr.u-tokyo.ac.jp/doc/sk/pub

[2] B. Pontecorvo, Zh. Eksp. Toer. Fiz. **53**, 1717 (1967) [Sov. Phys. JETP **26**, 984 (1968)]; V. Gribov and B. Pontecorvo, Phys. Lett. **28B**, 493 (1969).

[3] Y. Katayama, K. Matumoto, S. Tanaka, and E. Yamada, Prog. Theor. Phys. **28**, 675 (1962); Z. Maki, M. Nakagawa, and S. Sakata, *ibid.* **28**, 870 (1962).

[4] Super-Kamiokande Collaboration, F. Fukuda *et al.*, Phys. Rev. Lett. **81**, 1562 (1998).

[5] Super-Kamiokande Collaboration, F. Fukuda *et al.*, Phys. Lett. B **433**, 9 (1998).

[6] Super-Kamiokande Collaboration, F. Fukuda *et al.*, Phys. Lett. B **436**, 33 (1998).

[7] Super-Kamiokande Collaboration, F. Fukuda *et al.*, Phys. Rev. Lett. **82**, 2644 (1999).

[8] G. L. Fogli, E. Lisi, A. Marrone, and G. Scioscia, Phys. Rev. D **59**, 033001 (1999).

[9] Super-Kamiokande Collaboration, M. Messier, in *DPF'99*, Proceedings of the 1999 Meeting of the American Physical Society, Division of Particles and Fields, edited by K. Arisaka and Z. Bern (Library of the University of California at Los Angeles, Los Angeles, 1999). Transparencies available at http://www.physics.ucla.edu/dpf99

[10] Super-Kamiokande Collaboration, A. Habig, in *DPF'99* [9], hep-ex/9903047.

[11] MACRO Collaboration, M. Ambrosio *et al.*, Phys. Lett. B **434**, 451 (1998).

[12] Soudan-2 Collaboration, W. W. M. Allison *et al.*, Phys. Lett. B **449**, 137 (1999).

[13] Kamiokande Collaboration, S. Hatakeyama *et al.*, Phys. Rev. Lett. **81**, 2016 (1998).

[14] V. Barger, J. G. Learned, S. Pakvasa, and T. J. Weiler, Phys. Rev. Lett. **82**, 2640 (1999).

[15] P. Lipari and M. Lusignoli, Phys. Rev. D **60**), 013003 (1999).

[16] G. L. Fogli, E. Lisi, A. Marrone, and G. Scioscia, Phys. Rev. D **59**, 117303 (1999).

[17] T. Kajita, in Proceedings of the Workshop Future of Neutrino Physics, Institute of Cosmic Ray Research, Tokyo, Japan, 1999.

[18] Y. Grossman, Phys. Lett. B **359**, 141 (1995).

[19] L. M. Johnson and D. W. McKay, Phys. Lett. B **433**, 355 (1998).

[20] M. Gasperini, Phys. Rev. D **38**, 2635 (1988).

[21] M. Gasperini, Phys. Rev. D **39**, 3606 (1989).

[22] M. C. Gonzales-Garcia, M. M. Guzzo, P. I. Krastev, H. Nunokawa, O. L. G. Peres, V. Pleitez, J. F. W. Valle, and R. Zukanovich Funchal, Phys. Rev. Lett. **82**, 3202 (1999).

[23] V. DeSabbata and M. Gasperini, Nuovo Cimento A **65**, 479 (1981).

[24] M. Fukugita and T. Yanagida, Phys. Lett. B **206**, 93 (1988).

[25] D. V. Ahluwalia and T. Goldman, Phys. Rev. D **56**, 1698 (1997).

[26] S. Coleman and S. L. Glashow, Phys. Lett. B **405**, 249 (1997).

[27] S. L. Glashow, A. Halprin, P. I. Krastev, C. N. Leung, and J. Pantaleone, Phys. Rev. D **56**, 2433 (1997).

[28] S. Coleman and S. L. Glashow, Phys. Rev. D **59**, 116008 (1999).

[29] O.Yasuda, in *Proceedings of the Workshop on General Relativeity and Gravitation*, Tokyo, Japan, 1994, edited by K. Maeda, Y. Eriguchi, T. Futamase, H. Ishihara, Y. Kojima, and S. Yamada (Tokyo University, Japan, 1994), gr-qc/9403023, p. 510.

[30] J. Pantaleone, A. Halprin, and C. N. Leung, Phys. Rev. D **47**, 4199 (1993).

[31] A. Halprin, C. N. Leung, and J. Pantaleone, Phys. Rev. D **53**, 5365 (1996).

[32] R. Foot, C. N. Leung, and O. Yasuda, Phys. Lett. B **443**, 185 (1998).

[33] I. R. Kenyon, Phys. Lett. B **237**, 274 (1990).

[34] J. N. Bahcall, P. I. Krastev, and C. N. Leung, Phys. Rev. D **52**, 1770 (1995).

[35] J. R. Mureika, Phys. Rev. D **56**, 2408 (1997).

[36] T. Damour and A. M. Polyakov, Nucl. Phys. **B423**, 532 (1994).

[37] A. Halprin and C. N. Leung, Phys. Lett. B **416**, 361 (1998).

[38] D. Colladay and V. A. Kostelecky, Phys. Rev. D **55**, 6760 (1997); **58**, 116002 (1998).

[39] CPLEAR Collaboration, J. Ellis, N. E. Mavromatos, and D. V. Nanopoulos, hep-ex/9903005.

[40] A. Halprin and C. N. Leung, Phys. Rev. Lett. **67**, 1833 (1991).

[41] M. N. Butler, S. Nozawa, R. Malaney, and A. I. Boothroyd, Phys. Rev. D **47**, 2615 (1993).

[42] H. Minakata and H. Nunokawa, Phys. Rev. D **51**, 6625 (1995).

[43] J. R. Mureika and R. B. Mann, Phys. Lett. B **368**, 112 (1996).

[44] S. W. Mansour and T. K. Kuo, hep-ph/9810510.

[45] H. Casini, J. C. D'Olivo, R. Montemayor, and L. F. Urrutia, Phys. Rev. D **59**, 062001 (1999).

[46] R. B. Mann and U. Sarkar, Phys. Rev. Lett. **76**, 865 (1996).

[47] K. Iida, H. Minakata, and O. Yasuda, Mod. Phys. Lett. A **8**, 1037 (1993).

[48] H. V. Klapdor-Kleingrothaus, H. Päs, and U. Sarkar, Eur. Phys. J. A **5**, 3 (1999); see, however, A. Halprin and R. R. Volkas, hep-ph/9904298.